Water Policy 23 (2021) 750–764

Simulation and assessment of a water pollution accident caused by phenol leakage

Gaimei Guo[a,b,*] and Runbin Duan[a]

[a]*College of Environmental Science and Engineering, Taiyuan University of Technology, Taiyuan 030024, China*
**Corresponding author. E-mail: gmguo@126.com*
[b]*Shanxi Academy for Environmental Planning, Taiyuan 030024, China*

Abstract

Frequent occurrence of water pollution accidents has caused serious ecological and environmental damage. The purpose of this study was to assess the impacts of water pollution accidents on the human body and the ecosystem and to use a new calculation method of mean absolute deviation (MAD) to measure model error. A water pollution accident caused by the phenol leakage was simulated using the Environmental Damage Model of Water Pollution Accidents. In order to analyze the impacts of the phenol leakage event on the human body and the ecosystem, pollution level and its classification method were defined, and the result showed that the leakage event of phenol could have a destructive impact and present great danger in some areas, which covered 32–56% of the study area. The measurement of the model error indicated that lower resolution meant smaller MAD. Quantity Deviation and Hierarchical Deviation did not change with the resolution, and low resolution meant small Pixel Deviation. MAD not only reflected the deviation between layers but also embodied the impact of individual data on the whole deviation.

Keywords: Impact; Mean absolute deviation; Pollution levels; Resolution; Water pollution accidents

Highlights

- A new calculation method of mean absolute deviation is used to measure the model error.
- Lower resolution means smaller mean absolute deviation.
- Mean absolute deviation reflects the deviation between layers.
- The pollution level and its classification method are defined for the first time.
- The phenol leakage event causes destructive impacts and great dangers in some areas.

doi: 10.2166/wp.2021.153

1. Introduction

Currently, accidental pollution events such as process leaks, transport accidents, collisions and pipeline leaks occur frequently in many countries, such as the United States (Pulido-Velazquez & Ward, 2018) and China (Tang *et al*., 2018). Accidental pollution accidents can cause serious ecological and environmental damage to surrounding areas leading to an imbalance of the regional ecological system, and they have become a focus of public concern (Peng *et al*., 2017; Rui *et al*., 2017; Belayutham *et al*., 2018). Protecting the environment is a problem faced by every industry in the world. For example, the effects of the modern agriculture and irrigation system on the environment were studied (Valipour, 2016, 2017). In various pollution incidents, accidental water pollution incidents occur more and more frequently (He *et al*., 2011; Qu *et al*., 2018; Yang *et al*., 2019). Pollutants in water pollution accidents are various toxic organics, such as benzene, phenol, alcohol and so on. Phenol, as a typical organic matter, is highly toxic and corrosive (Li *et al*., 2018). It can enter the human body through the skin, esophagus and respiratory tract. Moreover, phenol can impact the central nervous system or damage liver and kidney function (Ren *et al*., 2017).

In recent years, the simulation of diffusion and transport processes of various pollutants under water pollution accidents has attracted worldwide attention (Yang *et al*., 2015; Tao *et al*., 2016). Most of these studies focus on the simulation of spatial–temporal change of pollutants by developing water quality models. For example, Ding *et al*. (2017) used a two-dimensional water quality model to simulate the change of pollutant concentration after accidental water pollution events. Dong *et al*. (2017) used a simulation software to predict the diffusion processes of pollutants and proposed an environmental risk assessment method in water pollution events. Ani *et al*. (2012) developed an analog system for simulating the pollutant migration process after water pollution events. Liu *et al*. (2016) deduced a formula for quantitative simulation of water pollution accidents. Grifoll *et al*. (2011) simulated the variation trend of pollutant concentration after accidental water pollution incidents. Wang *et al*. (2008) developed a water quality model to simulate the spatial–temporal change of pollutants in water pollution events. However, these studies still had two major limitations. One limitation is that few studies have defined pollution levels according to pollutant concentrations and have studied the impacts of water pollution accidents on the human body and the ecosystem, which are important for relevant departments to implement emergency contingency plans and to take corresponding measures. Another is that few analyses have used the appropriate method to measure model error. The novelties of the current study were to assess the impacts of water pollution events on the human body and the ecosystem based on pollution levels, and to use a new calculation method of mean absolute deviation (MAD) to measure model error, and applied it to a water pollution accident caused by the phenol leakage in Xinzhou, China.

2. Methodology and materials

2.1. Study area

The city of Xinzhou located in the north of Shanxi Province in China was taken as the study area (East longitude 110°53′ to 113°58′ and North latitude 38°37′ to 38°45′). Fen River is the main river in Shanxi Province flowing through Shanxi Province from north to south and emptying into the Yellow River. The Yellow River is the main source of drinking water in Shanxi Province. Phenol is

regarded as one of the most common organic pollutants in the world, and its standard concentration upper limit is set as 0.002 mg/L in the surface water in China including in the Yellow River. Characteristics of the Fen River are shown in Table 1.

2.2. The leakage event of phenol

At 16:56 pm on May 22, 2016, on the provincial highway S313, a tanker carrying 24.35 tons of phenol from Kelan to Shijiazhuang, Hebei Province, overturned in a traffic accident on the west road of Yaohui village in Jingle County, Xinzhou. As a result, the phenol leaked and about 5 tons of phenol flowed into Daya River along the drainage channel on the north side of the road. The leakage event of phenol was located in Jingle County, Xinzhou, Shanxi Province, China. The study area was from the accident site to the Liudu Bridge section.

2.3. Environmental damage model of water pollution accidents

In order to study the influence of the phenol leakage event on the downstream and banks of the Fen River, the Environmental Damage Model of Water Pollution Accidents was used to simulate the pollutant concentration. This model perfectly combines the most advanced calculation engine of hydrodynamic-water quality numerical simulation Delft3D-FLOW in the world with the standard 'the Map World' of China Bureau of Surveying and Mapping, and it can analyze and predict accidental water pollution events by drawing grids, setting parameters, calculating results and rendering.

2.4. A new calculation method of MAD

In general, there are several ways to measure model error, such as mean deviation (MD), root-mean-square error (RMSE) and MAD. The traditional calculation formula of MAD is given by the following equation:

$$MAD = \frac{\sum_{i=1}^{n} |Y_i - X_i|}{n} \tag{1}$$

Because MAD is an absolute value, it can avoid the problem that errors cancel each other out and reflect accurately the forecast error. Willmott & Matsuura (2006) argued that MD and MAD were

Table 1. Characteristics of Fen River.

No.	Index	Content
1	Name	Fen River
2	Province	Shanxi, China
3	Basin	The Yellow River Basin
4	Length	716 km
5	The basin area	39721 km^2
6	Water quality standard	Level – of GB3838-2002 (China)

more suitable than RMSE as a measure of average error because RMSE is a function of three characteristics of a set of errors rather than of one (the average error). Pontius *et al.* (2008) demonstrated by giving actual cases that MAD and MD could accurately measure error. Based on the traditional calculation formula of MAD, Willmott and Matsuura proposed a new calculation method of MAD. This method mainly considers the effects of resolution on MAD. Resolution is the number of pixels in each length direction times those in each width direction. For different resolutions, the value of MAD is different. In the new calculation method, MAD has three characteristic values including Quantity Deviation, Hierarchical Deviation and Pixel Deviation. The magnitude of MAD is determined by the three characteristic values. Pontius *et al.* (2008) used this new calculation method of MAD to measure the error of the Environmental Spatial–temporal Change Model. However, few studies have discussed the effects of resolution on Quantity Deviation, Hierarchical Deviation and Pixel Deviation and the effects of the three deviations on MAD. In this paper, the new calculation method of MAD was used to measure the errors of the Environmental Damage Model of Water Pollution Accidents.

2.4.1. Basic concepts. The new calculation method of MAD mainly considers the effect of resolution on MAD. When considering the resolution, MAD has three characteristic values, which are Quantity Deviation, Hierarchical Deviation and Pixel Deviation. MAD is the sum of the three values.

Quantity Deviation is the absolute value of the difference between the mean of X and the mean of Y.

Hierarchical Deviation (A) is the difference of regions according to different hierarchies.

Pixel Deviation (Pg) is the difference of pixel levels according to different hierarchies.

2.4.2. Calculation formula. The calculation formulas of Quantity Deviation, Hierarchical Deviation, Pixel Deviation and MAD are given as follows:

$$Q = \frac{\left|\sum_{s=1}^{S}\sum_{r=1}^{R1}\sum_{c=1}^{C1} Ds1_{rc}\right|}{N} \tag{2}$$

$$A = \frac{\sum_{s=1}^{S}\left|\sum_{r=1}^{R1}\sum_{c=1}^{C1} Ds1_{rc}\right|}{N} - Q \tag{3}$$

$$Pg = \frac{\sum_{s=1}^{S}\sum_{r=1}^{Rg}\sum_{c=1}^{Cg} |Dsg_{rc}|}{N} - A - Q \tag{4}$$

$$MAD = \frac{\sum_{s=1}^{S}\sum_{r=1}^{RG}\sum_{c=1}^{Cg} |Dsg_{rc}|}{N} \tag{5}$$

$$Dsg_{rc} = \sum_{i=g(r-1)+1}^{gr}\left[\sum_{j=g(c-1)+1}^{gc}(Ys_{ij} - Xs_{ij})\right] \tag{6}$$

The explanation is as follows: Dsg_{rc} is the pixel difference between row r and column c in the s hierarchy when the resolution is g, 1 is the original resolution, g is the resolution conversion factor, s is the hierarchy, X is the simulated data, Y is the monitoring data, r is the number of rows, c is the number of columns, and i and j are the number of rows and columns corresponding to the pixel when the original resolution is 1.

3. Results and discussion

3.1. Simulation results

According to pollutant diffusion time which is provided by Xinzhou Municipal Environmental Protection Bureau, phenol leakage was simulated for 48 h. The results were used to judge whether the exposure concentrations exceeded the surface water quality standard. Table 2 lists the area affected by phenol pollution at different instants after the release. The predicted pollution area expands from 7.24 km^2 after 2 h to 34.53 km^2 after 18 h, then decreases to 28.87 km^2 at 20 h, and finally decreases to 0.21 km^2 at 48 h.

3.2. The pollution level

3.2.1. The classification of the pollution level. In order to analyze the impact of the leakage event of phenol on the human body and the ecosystem, the pollution level is divided into four levels according to the concentration of phenol. The determination methods of these four levels are given as follows:

Level I: the pollutant concentration at the target point is lower than the safe concentration;
Level II: the pollutant concentration at the target point is higher than the safe concentration, but it falls into the lower one-quarter of the range between the safe concentration and the dangerous concentration;
Level III: the pollutant concentration at the target point falls into the range of one-quarter to one-half of the range between the safe concentration and the dangerous concentration; and
Level IV: the pollutant concentration at the target point falls into the range of higher than one-half of the range between the safe concentration and the dangerous concentration.

Table 2. Pollution areas of phenol at discrete intervals after the leakage event.

Time (h)	2	4	6	8	10	12
Area (km^2)	*7.24*	16.86	23.55	25.31	26.98	28.66
Time (h)	14	16	18	20	22	24
Area (km^2)	29.75	32.42	*34.53*	*28.87*	22.55	17.69
Time (h)	26	28	30	32	34	36
Area (km^2)	15.33	14.61	12.65	11.32	10.46	9.63
Time (h)	38	40	42	44	46	48
Area (km^2)	7.51	6.29	3.87	2.16	1.37	*0.21*

Italic values represent important data.

According to the above determination methods, the pollution levels of target points can be divided into the following four types:

Level I: safe, no human damage or ecosystem damage;
Level II: critical, likely to cause human injury and damage to major ecosystem;
Level III: dangerous, causing human injury and ecosystem damage; and
Level IV: destructive, resulting in death or disability and ecosystem destruction.

3.2.2. The pollution level of the phenol leakage event. Table 3 is the maximum phenol concentrations of all locations in the study area during the simulation time (48 h). In Table 3, when $12301047 < x < 12302007$, the maximum phenol concentration was 4.707–1.269 mg/L, which exceeds the danger concentration (0.04 mg/L) to a large extent. According to the determination methods of the pollution levels, the range of the phenol concentration for each level could be obtained (Table 4).

According to the maximum concentration of phenol at each position in the study area during the simulation time, the pollution levels are available for all positions. Figure 1 is the pollution levels in different areas (A, B, C and D). From Table 3, the range of A is $12301047 < x < 12404369$ and $4241921 < y < 4242803$. The range of B is $12404369 < x < 12518052$ and $4235562 < y < 4241921$. The range of C is $12518052 < x < 12519580$ and $4234657 < y < 4235562$. The range of D is $x > 12519580$ and $y < 4234657$.

As is seen from Figure 1, the pollution level in the 'blue' area is the highest (Level IV) and area A covers 13% of the study area, which can cause death or disability of people and ruin of the ecosystem. The 'red' area is considered to be at risk and covers 19% of it, which can cause harm to the human body and damage to the ecosystem. The 'green' area is in the critical state. The pollution level in the 'purple' area is the lowest (Level I) and area D covers 44% of it. Thus, it can be seen that the leakage event of phenol can cause a destructive impact and great danger in some areas which cover 32–56% of the study area, and relevant departments should launch emergency contingency plans and take corresponding measures to guarantee the safety of people's lives.

3.3. Application case

Nowadays, the sudden pollution incident has become one of the important reasons for the environmental damage. In order to effectively monitor and predict sudden pollution events, simulation software has become one of the important methods. In this paper, the Environmental Damage Model of Water Pollution Accidents was used to simulate a water pollution event, and the new calculation method of MAD was used to compare simulation data and monitoring data of the event to elaborate and analyze this new calculation method.

3.3.1. Uncertainty analysis. The monitoring data of the pollutant concentration in the accident were provided by Yuncheng Municipal Environmental Protection Bureau, and there were five monitoring sites. In this paper, the leakage point, Pujiang section and Liudu Bridge section were selected to calculate and analyze MAD. The three monitoring points are located at the starting end, the middle end and the end of the leakage, respectively. Table 5 shows the monitoring concentration and simulated concentration of the three monitoring sites. In Table 5, the maximum measured concentration was 5.815 mg/L

Table 3. The maximum phenol concentrations of all locations in the study area during the simulation time.

x-coordinate (m)	y-coordinate (m)	The maximum phenol concentrations (mg/L)
$x = 12301047$	$y = 4242803$	*4.707*
$x = 12301123$	$y = 4242759$	*4.125*
$x = 12301191$	$y = 4242706$	*3.862*
$x = 12301253$	$y = 4242669$	*3.796*
$x = 12301314$	$y = 4242618$	*2.835*
$x = 12301377$	$y = 4242551$	*2.524*
$x = 12301436$	$y = 4242483$	*2.192*
$x = 12301536$	$y = 4242336$	*2.573*
$x = 12301579$	$y = 4242259$	*2.678*
$x = 12301618$	$y = 4242185$	*1.867*
$x = 12301677$	$y = 4242043$	*1.880*
$x = 12301710$	$y = 4242016$	*1.549*
$x = 12301868$	$y = 4242015$	*1.117*
$x = 12301905$	$y = 4242001$	*1.598*
$x = 12301949$	$y = 4241985$	*1.435*
$x = 12302007$	$y = 4241982$	*1.269*
$12302007 < x < 12404369$	$4241921 < y < 4241982$	0.022–1.038
$x = 12404369$	$y = 4241921$	0.019
$x = 12404387$	$y = 4241918$	0.021
$x = 12404395$	$y = 4241913$	0.018
$x = 12404431$	$y = 4241905$	0.019
$x = 12404466$	$y = 4241899$	0.015
$x = 12404507$	$y = 4241885$	0.017
$x = 12404558$	$y = 4241876$	0.018
$x = 12404612$	$y = 4241755$	0.020
$x = 12404640$	$y = 4241732$	0.018
$x = 12404651$	$y = 4241674$	0.016
$x = 12404729$	$y = 4241619$	0.017
$x = 12404794$	$y = 4241603$	0.016
$x = 12404862$	$y = 4241558$	0.018
$12404862 < x < 12406793$	$4240165 < y < 4241558$	0.015–0.016
$x = 12406793$	$y = 4240165$	0.014
$x = 12407082$	$y = 4240158$	0.014
$x = 12407187$	$y = 4240152$	0.012
$x = 12407292$	$y = 4240143$	0.010
$x = 12407392$	$y = 4240088$	0.014
$x = 12407485$	$y = 4240054$	0.013
$x = 12407565$	$y = 4240051$	0.011
$x = 12407624$	$y = 4240019$	0.012
$x = 12407563$	$y = 4239857$	0.012
$12407563 < x < 12518052$	$4235562 < y < 4239857$	0.010–0.011
$x = 12518052$	$y = 4235562$	0.009
$x = 12518111$	$y = 4235554$	0.006
$x = 12518175$	$y = 4235526$	0.006
$x = 12518240$	$y = 4235458$	0.008
$x = 12518303$	$y = 4235412$	0.007

(*Continued.*)

Table 3. (*Continued.*)

x-coordinate (m)	*y*-coordinate (m)	The maximum phenol concentrations (mg/L)
$x = 12518368$	$y = 4235405$	0.006
$x = 12518439$	$y = 4235346$	0.009
$x = 12518518$	$y = 4235298$	0.008
$x = 12518611$	$y = 4235276$	0.005
$x = 12518736$	$y = 4235219$	0.008
$x = 12518886$	$y = 4235207$	0.006
$x = 12519037$	$y = 4235155$	0.004
$x = 12519171$	$y = 4235128$	0.002
$x = 12519280$	$y = 4235120$	0.003
$x = 12519367$	$y = 4235117$	0.002
$x = 12519443$	$y = 4235106$	0.002
$x = 12519512$	$y = 4234993$	0.001
$x = 12519580$	$y = 4234657$	0.001
$x > 12519580$	$y < 4234657$	0

Italic values represent important data.

Table 4. The range of the phenol concentration for each pollution level.

The pollution level	The safe concentration (mg/L)	The dangerous concentration (mg/L)	The range of the phenol concentration *R* (mg/L)
Level I	0	0.04	$R \leq 0$
Level II	0	0.04	$0 < R \leq 0.01$
Level III	0	0.04	$0.01 < R \leq 0.02$
Level IV	0	0.04	$R > 0.02$

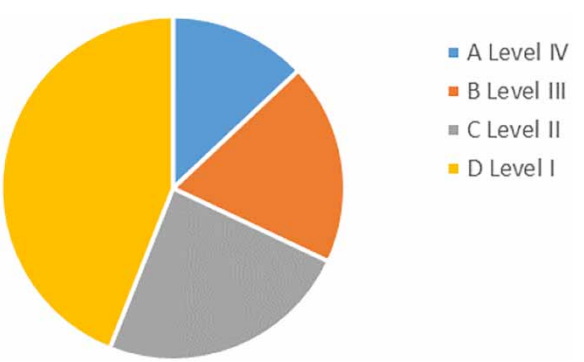

Fig. 1. The pollution levels in different areas in the study area during the simulation time (area A, B, C and D cover 13, 19, 24 and 44% of the study area, respectively (13% + 19% + 24% + 44% = 100%). Please refer to the online version of this paper to see this figure in colour: http://dx.doi.org/10.2166/wp.2021.153.

Table 5. The monitoring concentrations and simulated concentrations of phenol.

Name of monitoring station	Leakage time (h)	Monitoring concentration (mg/L)	Simulated concentration (mg/L)	Uncertainty (U)
The leakage point	2	3.895	3.269	0.16
	4	4.163	3.163	0.24
	6	*5.815*	*4.707*	0.19
	8	3.124	3.421	0.10
	10	2.111	1.998	0.05
	12	1.238	1.465	0.18
	14	0.754	0.854	0.13
	16	0.861	0.620	0.28
	18	0.027	0.018	0.33
	20	0.015	0.018	*0.20*
	22	0.021	0.023	0.10
	24	0.022	0.024	0.09
	26	0.013	0.012	0.08
	28	0.015	0.016	0.07
	30	0.023	0.018	0.22
	32	0.008	0.006	*0.25*
	34	0.012	0.009	*0.25*
	36	0.009	0.011	0.22
	38	0.008	0.012	0.50
	40	0.011	0.008	0.27
	42	0.006	0.006	0.00
	44	0.005	0.007	0.40
	46	0.007	0.005	0.29
	48	0.004	0.003	*0.25*
Pujiang section	2	0.001	0.001	0.00
	4	0.133	0.147	0.11
	6	1.124	1.216	0.08
	8	0.128	0.141	0.10
	10	1.258	1.782	0.42
	12	2.116	1.923	0.09
	14	2.051	1.761	0.14
	16	0.362	0.293	0.19
	18	0.352	0.253	0.28
	20	0.051	0.046	0.10
	22	0.591	0.475	*0.20*
	24	0.201	0.215	0.07
	26	0.042	0.047	0.12
	28	0.235	0.157	0.33
	30	0.406	0.292	0.28
	32	0.051	0.046	0.10
	34	0.066	0.067	0.02
	36	0.077	0.067	0.13
	38	0.104	0.123	0.18
	40	0.079	0.091	0.15
	42	0.074	0.078	0.05
	44	0.058	0.056	0.03
	46	0.052	0.044	0.15
	48	0.105	0.079	*0.25*

(*Continued.*)

Table 5. (*Continued.*)

Name of monitoring station	Leakage time (h)	Monitoring concentration (mg/L)	Simulated concentration (mg/L)	Uncertainty (U)
Liudu Bridge section	*2*	*0.000*	*0.000*	–
	4	0.000	0.003	–
	6	0.000	0.005	–
	8	0.000	0.008	–
	10	0.000	0.010	–
	12	0.000	0.008	–
	14	0.000	0.007	–
	16	0.000	0.009	–
	18	0.000	0.010	–
	20	0.000	0.013	–
	22	0.000	0.019	–
	24	0.000	0.029	–
	26	0.000	0.045	–
	28	0.077	0.063	0.18
	30	0.148	0.129	0.13
	32	0.023	0.027	0.17
	34	0.349	0.411	0.18
	36	0.740	0.636	0.14
	38	0.972	0.864	0.11
	40	0.886	1.007	0.14
	42	0.453	0.399	0.12
	44	0.164	0.124	0.24
	46	0.052	0.059	0.13
	48	0.042	0.047	0.12

Italic values represent important data.

and the maximum simulated concentration was 4.707 mg/L when leakage time was 6 h at the leakage point. The minimum measured concentration was 0.000 mg/L and the minimum simulated concentration was 0.000 mg/L when leakage time was 2 h at the Liudu Bridge section. At the same time, uncertainty (U) is calculated by comparing the measured concentration with the simulated concentration. The calculation formula is given as follows:

$$U = |\text{simulated concentration} - \text{measured concentration}|/\text{measured concentration} \quad (7)$$

The smaller values of uncertainty mean that the simulated concentrations are closer to the measured concentrations indicating the better simulation results. There are 41 U values less than 0.20 in 59 U values in Table 5, that is 69% in the whole numbers of the U values, while 48 U values less than 0.25 account for 81% of the whole numbers of the U values. It shows that the model used in this study has high accuracy and the simulation results are relatively reliable.

3.3.2. The effect of resolution on MAD. In this case, the changes in resolution were achieved by averaging the original resolution at two points. Table 6 is the effects of resolution on MAD. It showed that

Table 6. The effect of resolution on MAD.

Name of monitoring station	Resolution	MAD
The leakage point	*1*	*0.2781*
	0.5	*0.1704*
Pujiang section	1	0.1425
	0.5	0.1230
Liudu Bridge section	1	0.0443
	0.5	0.0227

Italic values represent important data.

lower resolution meant smaller MAD. For example, MAD was 0.1704 when the resolution was 0.5, and MAD was 0.2781 when the resolution was 1 at the leakage point.

3.3.3. The effect of resolution on each deviation and the effect of each deviation on MAD. In this paper, MAD consisted of three parts: Quantity Deviation, Hierarchical Deviation and Pixel Deviation. This section would analyze the effects of resolution on each deviation and the effects of each deviation on MAD. This paper compared the components of MAD with a column chart of deviation accumulation. In Figures 2–4, vertical axis represents MAD. The horizontal axis represents the resolution. Blue represents Quantity Deviation. Red represents Hierarchical Deviation. Green represents Pixel Deviation. The stack bar charts on the left showed the calculation results of each deviation when the resolution was 1. The stack bar charts on the right showed the calculation results of each deviation when the resolution was 0.5.

The above column charts of deviation accumulation showed the components of MAD and directly reflected the proportion of each deviation. Table 7 is the calculation results of each deviation at different resolutions.

The difference between the monitoring concentration and simulated concentration can be clearly understood by calculating Quantity Deviation. It is not only an intuitive index to analyze the deviation but also an important index to distinguish the deviation. Table 7 shows that Quantity Deviation did not change with the resolution, and Quantity Deviation was always positive. Meanwhile, smaller Quantity meant better simulation effects. For example, Quantity Deviation at the Liudu Bridge section was the smallest

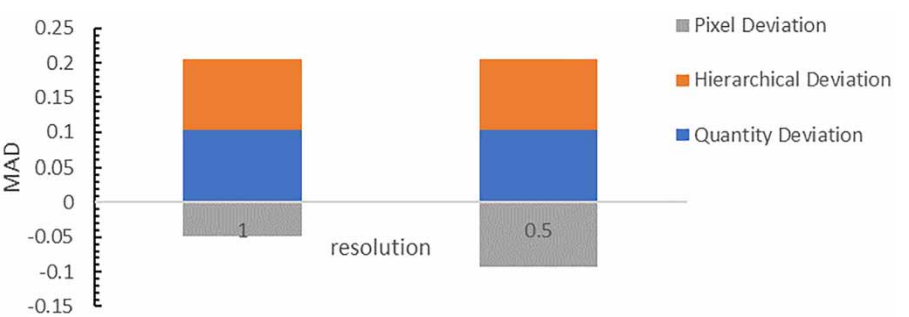

Fig. 2. The effect of resolution on MAD at the leakage point. Please refer to the online version of this paper to see this figure in colour: http://dx.doi.org/10.2166/wp.2021.153.

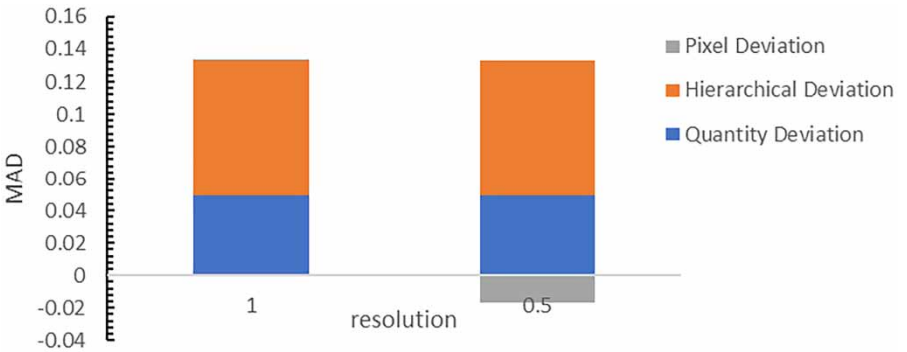

Fig. 3. The effect of resolution on MAD at the Pujiang section. Please refer to the online version of this paper to see this figure in colour: http://dx.doi.org/10.2166/wp.2021.153.

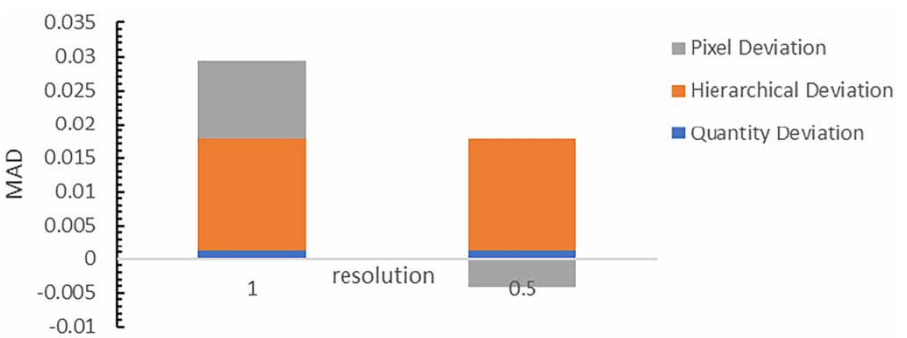

Fig. 4. The effect of resolution on MAD at the Liudu Bridge section. Please refer to the online version of this paper to see this figure in colour: http://dx.doi.org/10.2166/wp.2021.153.

Table 7. The calculation results of each deviation at different resolutions.

Name of monitoring station	Resolution	Quantity Deviation	Hierarchical Deviation	Pixel Deviation
The leakage point	1	0.1027	0.1027	*− 0.0493*
	0.5	0.1027	0.1027	*− 0.0924*
Pujiang section	1	0.0496	*0.0834*	0.0009
	0.5	0.0496	*0.0834*	−0.0170
Liudu Bridge section	1	*0.0012*	0.0167	0.0115
	0.5	*0.0012*	0.0167	−0.0041

Italic values represent important data.

(0.0012), and the simulated concentration was closest to the monitored concentration. In addition to Quantity Deviation, there was also Hierarchical Deviation that caused errors in the simulation results, which represented the inconsistency caused by the deviation between layers. Hierarchical Deviation did not change with the resolution because Quantity Deviation in each layer was independent of the resolution, and stratification did not change with the resolution. For example, Hierarchical Deviation at the Pujiang

section was 0.0834 whether the resolution was 1 or 0.5. Hierarchical Deviation was to use the sum of Quantity Deviation at different levels minus the component Quantity Deviation of this set of data to calculate the component of the additional deviation. The third factor causing the deviation was Pixel Deviation. The monitoring concentration at different times was averaged to form a data combination with different resolutions for analysis. The results showed that low resolution meant small Pixel Deviation. For example, Pixel Deviation was −0.0493 when resolution was 1 and it was −0.0924 when resolution was 0.5 at the leakage point. It was because when the resolution was smaller, pixels were neutralized and the difference value of each pixel point was reduced due to neutralization. Therefore, the simulated concentration was closer to the monitoring concentration.

3.3.4. The advantage of MAD. This section discusses the advantages of MAD by comparing MAD with MD. The formula for calculating MD is given as follows. Equation (8) was used to calculate the MD of the three monitoring points at different resolutions, and the results are shown in Table 8.

$$MD = \frac{\sum_{i=1}^{n} (Y_i - X_i)}{n} \tag{8}$$

It is seen from Table 8 that MD did not distinguish positive and negative data, but calculated the deviation by direct accumulation and equalization. Therefore, analyzing data with MD can represent the deviation between the overall simulated data and the monitoring data, but it had no sense in analyzing the deviation of individual data. However, MAD is composed of three parts. Among them, Quantity Deviation can represent the difference between all simulation data and the monitoring data. Hierarchical Deviation can stratify the data to reflect the deviation between layers. Pixel Deviation can analyze the difference between the monitoring data and the simulated data by changing the resolution and reflect the impact of extreme deviations on the overall simulation results. In short, compared with MD, MAD not only reflected the deviation between layers but also embodied the impact of individual data on the whole deviation.

4. Conclusions

One advantage of this study was that it assessed the impacts of water pollution accidents on the human body and the ecosystem, which is important for relevant departments to take corresponding

Table 8. The calculation results of MD.

Name of monitoring station	Resolution	MD
The leakage point	1	−0.1028
	0.5	−0.1028
Pujiang section	1	0.0496
	0.5	0.0496
Liudu Bridge section	1	0.0012
	0.5	0.0012

measures. Meanwhile, the new calculation method of MAD was used to measure model errors. This has rarely been mentioned in previous studies. The leakage event of phenol in Xinzhou, China, was used as a case study. On the one hand, according to the pollution levels proposed in this paper, the leakage event of phenol could cause a destructive impact and great danger in some regions which covered 32–56% of the study area, and related departments should launch emergency contingency plans. On the other hand, the measurement of the model errors indicated that lower resolution meant smaller MAD. Meanwhile, Quantity Deviation and Hierarchical Deviation did not change with the resolution, and low resolution meant small Pixel Deviation. Furthermore, Quantity Deviation can represent the difference between all simulation data and the monitoring data. Hierarchical Deviation can stratify the data to reflect the deviation between layers. Pixel Deviation can analyze the difference between the monitoring data and the simulated data by changing the resolution and reflect the impact of extreme deviations on the overall simulation results. In a word, MAD not only reflected the deviation between layers, but also embodied the impact of individual data on the whole deviation.

In summary, this study is the first attempt to define pollution levels according to pollutant concentrations and analyze the effects of resolution on quantity deviation, hierarchical deviation and pixel deviation. The results will be used to determine when an exposure has happened to a receptor and how bad it will be in the future. This not only provides a scientific basis for the risk assessment but also supports an early warning and emergency response. However, the limitation of this model was that river flow was fixed, but it was affected by weather, season and other factors during the pollution process. So, simulation results had certain errors. In future studies, the simulation system should be improved to some extent. For example, the flow rate, slope and river section should be set as the parameters of the system, and the value of parameters should be set as dynamic, so that the simulation results would be more reliable and the environmental damage caused by water pollution events can be more accurately analyzed.

Acknowledgements

We are very grateful to Ms Lihua Wang in Shanxi Academy for Environmental Planning, Taiyuan, China, and Mr Chongzheng Zhao and Ms Lin Lv at Taiyuan University of Technology, Taiyuan, China, for their kind cooperation and discussion at different stages of this study and their timely efforts in supplying the data and information needed for this study.

Data availability statement

All relevant data are included in the paper or its Supplementary Information.

References

Ani, E. C., Agachi, P. S. & Cristea, M. V. (2012). Mathematical models to support pollution counteraction in case of accidents. *Environ. Eng. Manag. J. 16*(1), 143–151.

Belayutham, S., González, V. A. & Yiu, T. W. (2018). The dynamics of proximal and distal factors in construction site water pollution. *J. Cleaner Prod. 113*, 54–65.

Ding, X. W., Wang, S. Y., Jiang, G. H. & Huang, G. H. (2017). A simulation program on change trend of pollutant concentration under water pollution accidents and its application in Heshangshan drinking water source area. *J. Cleaner Prod. 167*(5), 326–336.

Dong, L., Liu, J., Du, X., Dai, C. & Liu, R. (2017). Simulation-based risk analysis of water pollution accidents combining multi-stressors and multi-receptors in a coastal watershed. *Ecol. Indic. 62*(7), 154–163.

Grifoll, M., Jordá, G., Espino, M., Romo, J. & García-Sotillo, M. (2011). A management system for accidental water pollution risk in a harbor: the Barcelona case study. *J. Mar. Syst. 88*(1), 60–73.

He, Q., Peng, S., Zhai, J. & Xiao, H. W. (2011). Development and application of a water pollution emergency response system for the Three Gorges Reservoir in the Yangtze River, China. *J. Environ. Sci. 23*(4), 595–600.

Li, J. F., Zhang, B., Liu, M. & Wang, Y. (2018). Numerical simulation of the large-scale malignant environmental pollution incident. *Process Saf. Environ. 87*(4), 232–244.

Liu, R. Z., Borthwick, G. L., Lan, D. D. & Zeng, W. H. (2016). Environmental risk mapping of accidental pollution and its zonal prevention in a city. *Process Saf. Environ. 91*(8), 397–404.

Peng, J., Song, Y., Yuan, P., Xiao, S. & Han, L. (2017). A novel identification method of the environmental risk sources for surface water pollution accidents in chemical industrial parks. *J. Environ. Sci. 25*(7), 1441–1449.

Pontius Jr., R. G., Olufunmilayo, T. & Chen, H. (2008). Components of information for multiple resolution comparison between maps that share a real variable. *Environ. Ecol. Stat. 15*(2), 111–142.

Pulido-Velazquez, M. & Ward, F. A. (2018). Comparison of water management institutions and approaches in the United States and Europe – what can we learn from each other. In *Competition for Water Resources* (Chapter 3.3) (G. Kortun ed.), pp. 423–441.

Qu, J. H., Meng, X. L. & You, H. (2018). Multi-stage ranking of emergency technology alternatives for water source pollution accidents using a fuzzy group decision making tool. *J. Hazard. Mater. 310*, 68–74.

Ren, L. F., Chen, R., Zhang, X. F., Shao, J. H. & He, Y. L. (2017). Phenol biodegradation and microbial community dynamics in extractive membrane bioreactor (EMBR) for phenol-laden saline wastewater. *Bioresour. Technol. 244*(1), 1121–1128.

Rui, Y., Shen, D., Khalid, S., Yang, Z. & Wang, J. (2017). GIS-based emergency response system for sudden water pollution accidents. *Phys. Chem. Earth, Parts A/B/C 82*, 115–121.

Tang, C., Yi, Y., Yang, Z. & Cheng, X. (2018). Water pollution risk simulation and prediction in the main canal of the South-to-North water transfer project. *J. Hydrol. 519*, 2111–2120.

Tao, Y., Ren, H. T. & Xia, J. X. (2016). Investigation on disposal effect of different countermeasure of sudden water pollution accident. *J. Basic Sci. Eng. 21*(2), 203–213.

Valipour, M. (2016). How do different factors impact agricultural water management? *Open Agri. 1*, 89–111.

Valipour, M. (2017). Global experience on irrigation management under different scenarios. *J. Water Land Dev. 32*(I–III), 95–102.

Wang, Q. G., Zhao, X. H. & Wu, W. J. (2008). Advection-diffusion models establishment of water-pollution accident in middle and lower reaches of Hangjiang River. *Adv. Water Sci. 19*(4), 500–504.

Willmott, C. J. & Matsuura, K. (2006). On the use of dimensioned measures of error to evaluate the performance of spatial interpolators. *Int. J. Geogr. Inf. Sci. 20*(1), 89–102.

Yang, W., Song, J., Higano, Y. & Tang, J. (2015). Exploration and assessment of optimal policy combination for total water pollution control with a dynamic simulation model. *J. Cleaner Prod. 102*, 342–352.

Yang, L. K., Peng, S., Zhao, X. H. & Li, X. (2019). Development of a two-dimensional eutrophication model in an urban lake (China) and the application of uncertainty analysis. *Ecol. Modell. 345*, 63–74.

Received 28 July 2020; accepted in revised form 26 March 2021. Available online 26 April 2021